$CaCu_3Ti_4O_{12}$: Pressure dependence of electronic and vibrational structures

Journal of Physics: Conference Series **1609** (2020) 012005 doi:10.1088/1742-6596/1609/1/012005

$CaCu_3Ti_4O_{12}$: Pressure dependence of electronic and vibrational structures

E. Jara[1], F. Aguado[1], J. González[1], R. Valiente[2] and F. Rodríguez[1]

[1]MALTA TEAM, DCITIMAC, Facultad de Ciencias, Universidad de Cantabria, 39005 Santander, Spain.

[2]Nanomedicine Group-IDIVAL, Dpto. Física Aplicada, Facultad de Ciencias, Universidad de Cantabria, 39005 Santander, Spain.

E-mail: fernando.rodriguez@unican.es

Abstract. The effects of pressure in electronic and vibrational properties of the double perovskite $CaCu_3Ti_4O_{12}$ have been investigated in the 0-25 GPa range by optical absorption and Raman spectroscopy. Besides a full structural characterization, we aim at unveiling whether the ambient $Im\bar{3}$ crystal structure is stable under high pressure conditions and how its giant dielectric permitivity and electronic gap varies with pressure. Results show that there is evidence of neither structural phase transition nor metallization in $CaCu_3Ti_4O_{12}$ in the explored pressure range. We have observed the eight Raman active modes associated with its $Im\bar{3}$ crystal phase and obtained their corresponding frequency and pressure shift. Moreover, the direct electronic band gap (2.20 eV), which is mainly associated with the oxygen-to-copper charge transfer states, increases slightly with pressure at a rate of 13 meV GPa^{-1} from 0 to 10 GPa. Above this pressure is almost constant (E_g = 2.3 eV). The results highlight the high stability of the compound in its $Im\bar{3}$ phase against compression.

1. Introduction

$CaCu_3Ti_4O_{12}$ (CCTO) is a double perovskite oxide which acquired interest due to its giant dielectric permittivity (16000-18000) at ambient conditions [1, 2, 3]. Actually, it is not only at room temperature, but its permittivity remains almost constant over a wide temperature (100-700 K) and frequency (0–10^6 Hz) ranges [4]. The origin of its unexpected huge dielectric constant is still a mystery for which many models have been proposed [1, 2, 3, 4]. Recent studies relate this behavior to extrinsic factors such as defects and the creation of barrier layer capacitances at twin boundaries [1]. First-principles DFT calculations suggest that it could be related to lattice effects [5, 6], however, the obtained permittivity is much lower than the observed experimentally. Experiments on thin films of CCTO showed a low frequency permittivity of about 10^8 [7], that supports the hypothesis of extrinsic defects as the main cause for the giant dielectric constant. Furthermore, the observation of small length scale twinning in CCTO single crystals [1] is also consistent with this hypothesis.

CCTO belongs to the family of $ACu_3Ti_4O_{12}$ (A = Ca, Sr, Ba, $Bi_{2/3}$, $Y_{2/3}$, $La_{2/3}$) double-perovskite-type oxide [1], space group $Im\bar{3}$ at ambient conditions, where Ca^{2+} and Cu^{2+} ions are ordered on site A, and Ti^{4+} is located on site B of the ABO_3 perovskite structure. Interestingly, Cu^{2+} shows a Jahn-Teller distortion tilting the TiO_6 octahedra. Thanks to the double perovskite structure, this material accommodates both Ti^{4+} and the open-shell Cu^{2+} in the lattice sites

providing, respectively, photocatalitic and electronic gap reduction in this material. In addition, its high dielectric permittivity makes it promising for microelectronics. Since TiO_2 is an efficient UV-active photocatalyst and CuO is an efficient visible light absorber, the combination of both in the same crystal structure enhances its visible light photocatalytic activity [8]. Also, CCTO shows a polycrystalline porous nanostructures being of interest for gas and biochemical sensing.

The application of pressure to CCTO allows us to explore phase stability and how it affects its mechanical, electrical and optical properties. We are interested in the pressure-dependence of Raman modes to clarify the vibrational structure of this compound. Previous Raman [9, 23], x-ray diffraction [9], electrical condutivity as a function of temperature and pressure together with DFT calculations [22] report contradictory results about phase transformation and pressure-induced metallization deserving clarification. Firstly, studies in the 10 and 600 K range [4] or as a function of pressure (up to 5.3 GPa [9] or up to 20 GPa [23]), reported different Raman mode structure and associated frequencies. Secondly, there is a lack of consensus about structural transformations induced by pressure. Whether pressure induces a cubic ($Im\overline{3}$) to rhombohedral ($R\overline{3}$) phase transition around 3-4 GPa as predicted by DFT following a metallization (gap closure) between 6 and 7 GPa [22], or there is an iso-structural phase transition between 8 and 9 GPa as deduced by Raman spectroscopy in the 0-20 GPa range with no sign of metallization [23]) are contradictory results deserving clarification.
Our main goal is to investigate on the stability of the the ambient-pressure cubic phase$Im\overline{3}$ together with the behavior of the electronic gap under high-pressure conditions. An important aspect is to use single-phase synthesized CCTO samples, enabling to measure the band gap as a function of pressure and check whether it reduces with pressure yielding metallization, or remains insulator from 0 to 25 GPa.

2. Experimental

CCTO powder has been synthesized by the solid state reaction method [10, 11] using $CaCO_3$, CuO and TiO_2 as precursors. The precursors have been air milled for 24 h, using a planetary mill equipped with a container and balls made both of zircon, and operating at 250 rpm with a ball ratio of 1/10. The resultant powder was then pressed into pellets under 5-ton loading (about 0.5 GPa). In order to get an homogeneous structural sample, the pellet was subjected to a thermal treatment in air using an electrical oven. The method consisted of heating the sample slowly (3 ^{o}C/min) up to 500 ^{o}C for 2 h. Then, it was heated again (3 ^{o}C/min) up to 850^{o}C for 1 h, following a further heating (4 ^{o}C/min) up to 1100 ^{o}C, at which temperature the sample was annealed for 24 h. After this treatment the sample was cooled gradually down to room temperature. The structure at ambient pressure, $Im\overline{3}$ space group, was checked by powder X-ray diffraction (XRD) using a Bruker D8 diffractometer, and analyzed by a TOPAS software. The obtained powder x-ray diffractogram was accounted for on the basis of a cubic structure ($Im\overline{3}$ space group) with a cell parameter $a = 7.394(2)$ Åat ambient conditions. No sign of impurities and other phase formation was found within the experimental uncertainty.

We used a four-post diamond anvil cell (DAC) and a membrane DAC for optical absorption and Raman spectroscopy. 200-μm-thick Inconel 625 gaskets were preindented to reduce thickness down to 40 μm. Then, suitable 200-μm-diameter holes were perforated with a BETSA motorized electrical discharge machine. Spectroscopic paraffin oil (Merck spectroscopic grade) was used as pressure transmitting media. It must be noted that according to the ruby line broadening, nonhydrostatic effects were significant in the explored range, as previously reported [12].

The diffuse reflectance spectra were obtained using a Cary 6000i UV-Vis-NIR spectrophotometer equipped with an integrating sphere over the 200-1700 nm range. Since the CCTO is almost black, for room temperature optical absorption, we made a thin pellet by pressing the powder in the DAC. This way allows us to get measurable transmitted light through the sample for absorption under high-pressure conditions. The experimental setup for optical absorption

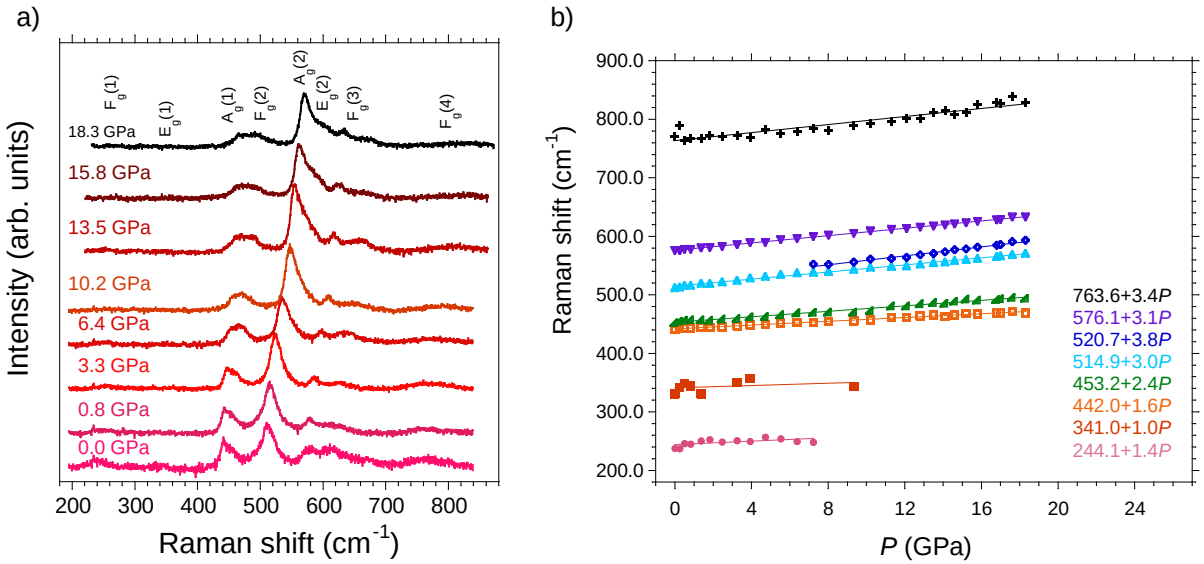

Figure 1. a) Pressure dependence of the Raman spectrum of CCTO. The spectra show the eight peaks which are associated to the corresponding Raman active modes of the $Im\bar{3}$ phase. b) Variation of the vibrational frequencies with pressure for the eight Raman modes. The equations obtained by least-squares linear fits to the experimental frequencies as $\omega(P) = \omega_0 + (d\omega/dP)P$, in the $Im\bar{3}$ phase are shown. Frequencies and corresponding pressure rates and Grüneisen parameters are collected in Table 1.

has been described elsewhere [13, 15]. Vis-NIR absorption data were obtained by using an Ocean Optics USB 2000+ spectrometer and a NIRQUEST 512 spectrometer, respectively. The Raman spectra were taken from the powder with a Horiba T64000 triple spectrometer using the 514.5-nm line of a Coherent Innova Spectrum 70 Ar^+ -Kr^+ laser and nitrogen-cooled CCD (Jobin-Yvon Symphony) with a confocal microscope operating with a Mitutoyo 20× and 50× objectives.

3. Results and discussion

3.1. Raman spectra

Figure 1 shows the variation of the Raman spectrum of CCTO with pressure up to 18.3 GPa, in this pressure range no phase transition was detected. Peak frequencies and mode assignment are collected in Table 1. Mode assignment was done following previous measurements reported elsewhere [4, 9]. We observe all eight Raman active modes expected for the $Im\bar{3}$ phase. Peaks at 244.1, 341.0, 442.0, 453.2, 514.9 and 520.7 cm^{-1} correspond to TiO_6 rotation-like modes, whereas peaks at 576.1 and 763.6 cm^{-1} correspond to Ti-O-Ti anti-symmetric and symmetric (breathing) stretching modes of the TiO_6 octahedron, respectively. The intensity of the $F_g(1)$ (244.1 cm^{-1}) and $E_g(1)$ (341.0 cm^{-1}) modes is too weak to get suitable values of their pressure shift above 10 GPa. The $A_g(2)$ mode (514.9 cm^{-1}) appears like the most prominent peak in the Raman spectrum. Upon pressure, we detect another mode which appears as a shoulder of the $A_g(2)$ peak. Its blueshift pressure rate is faster than the $A_g(2)$ pressure rate (Figure 1). We associate this shoulder to the $E_g(2)$ mode that can be clearly identified above 7 GPa. We estimate a frequency of 520 cm^{-1} at ambient pressure by extrapolating the linear fit $\omega(P)$ to zero pressure.

From the pressure dependence of the Raman spectrum no evidence of structural phase

Mode	ω_V (cm^{-1})	ω_K (cm^{-1})	LDC (cm^{-1})	ω_0 (cm^{-1})	$\gamma = (K_0/\omega)\ d\omega/dp$
$F_g(1)$	-	292	280	244.1	1.16
$E_g(1)$	-	-	318	341.0	0.59
$A_g(1)$	444	445	428	442.0	0.73
$F_g(2)$	453	400?	405	453.2	1.07
$A_g(2)$	510	511	512	514.9	1.17
$E_g(2)$	-	499	548	520.7	1.48
$F_g(3)$	576	575	574	576.1	1.09
$F_g(4)$	761	-	708	763.6	0.90

Table 1. Raman mode frequencies and Grüneisen parameters of CCTO ($Im\overline{3}$ phase) measured in this work, ω_0, compared with those obtained by Valim (ω_V) [9] and Kolev (ω_K) [4]. LCD corresponds to the calculated frequencies using lattice-dynamics methods [4]. Grüneisen parameters γ were derived from the frequency and pressure coefficient values from Fig. 1 using a CCTO bulk modulus of $K_0 = 212$ GPa (with fixed $K_0' = 4$) [9].

.

transition was found up to 18 GPa, thus stressing the stability of the $Im\overline{3}$ phase in this range. All Raman frequencies increase linearly upon increasing pressure, at rates ranging from 1.0 to 3.8 cm^{-1} GPa^{-1} (Table 1). It must be noted that previous works in CCTO [9] report a negative pressure shift coefficient ($\alpha < 0$) for the highest frequency $F_g(4)$ breathing mode at 763.6 cm^{-1} in contrast to the positive sign reported in this work (Fig. 1), which shows one of the highest positive pressure shifts ($\alpha = 3.4$ cm^{-1} GPa^{-1})). The existence of possible crystal instabilities in previous works is likely but no information about it is provided in [9]. The Grüneisen parameters given in Table 1 have been obtained using a bulk modulus of 212 GPa [16, 9]. These values for the stretching modes are close to 1 thus being consistently with other experimental and calculated values typically reported for stretching modes. γ values of 1.5 and 1.1 have been derived for the highest stretching vibrations in TiO_2 using α and K_0 values reported for rutile [20, 21, 19] and anatase [17, 18], respectively. The slightly smaller γ and higher frequency ω_0 measured in CCTO indicate that Ti-O bonds in CCTO are probably tougher than Ti-O bonds in rutile and anatase TiO_2 phases.

3.2. Electronic structure, reflectance and optical absorption

Figure 2 shows the diffuse reflectance spectrum of CCTO at ambient conditions, with $F(R)$ being the Kubelka-Munk function ($F(R)$=(1-R)^2/2R), with $R(\lambda) = I(\lambda)/I_0(\lambda)$ being the integrated reflectance signal. The spectrum shows a complex band structure which is basically related to internal Cu^{2+} crystal-field excitations and O^{2-} to Cu^{2+} charge-transfer (CT) transitions, and band gap excitation involving Ti^{4+} conduction band states. In particular, we associate the band at 1.5 eV to internal Cu^{2+} ($d-d$) transitions within a square planar coordination (D_{4h}). The higher energy band, between 2 and 4 eV corresponds to CT transitions from $O^{2-}(2p)$ valence orbitals to $Cu^{2+}(3d)$ intermediate band. Bands located above 4 eV correspond to band-gap transitions (CT-like) to the Ti^{4+} (t_{2g} and e_g; O_h notation) conduction band states [8]. We have explored the variation of the CT band-gap edge as a function of the photon energy in detail by plotting $[F(R) \times E]^n$ vs E in order to unveil the direct (n=2) –or indirect(n=1/2)– type behavior of the absorption edge. The analysis indicates that both plots show a linear dependence, providing gap energies of $E_g = 2.09$ eV for direct gap transition and $E_g = 1.42$ eV for indirect gap.

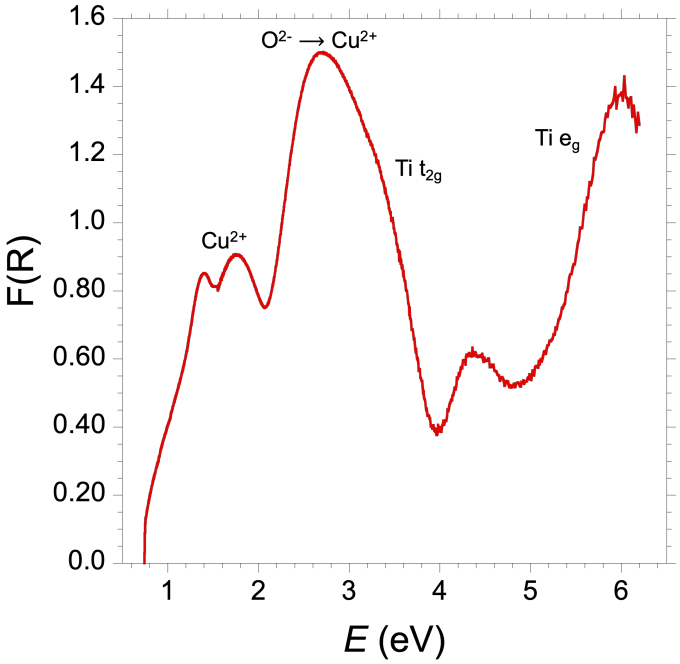

Figure 2. Diffuse reflectance spectrum of CCTO at ambient conditions. The band below 2 eV corresponds to internal Cu^{2+} $(d-d)$ transitions (D_{4h}). The band between 2 and 4 eV corresponds to CT transitions from $O^{2-}(2p)$ valence orbitals to $Cu^{2+}(3d)$, and those above 4 eV correspond to band-gap transitions to the $Ti^{4+}(t_{2g}$ and e_g; O_h notation) conduction-band states.

We have also investigated the optical absorption spectrum of a DAC-pressed CCTO powder sample near the band gap edge (Fig. 3), which is quite challenging due to its intense dark colour (blackish) even working with 20μm-thick samples. Nevertheless, this absorption-based method provides more suitable data for band gap analysis and thus of the gap energy. At ambient pressure, we measured a CT band gap of $E_g = 2.2$ eV for direct gap and $E_g = 1.6$ eV for indirect gap. It must be noted that there is a slight difference with E_g values obtained through the diffuse reflectance spectra. However, the absorption E_g values are in good agreement with those reported elsewhere [8]. Pressure measurements show that the CT band gap doesn't vary very much with pressure stressing the stability of the crystal structure and electronic band gap from 0 to 25 GPa range. The direct band gap increases linearly at a rate of about 13 meV GPa^{-1} from 0 to 10 GPa, and remains almost constant in the 10 - 25 GPa range. This result clarifies the electronic structure of CCTO, and shows that there is no CT band gap closure in this pressure range, in contrast to expectations on the basis of DFT results reported elsewhere [22].

4. Conclusions

We have shown that the electronic and vibrational structures of CCTO do change smoothly with pressure from 0 to 25 GPa range, thus indicating a high stability against compression. We have identified the eight Raman active modes consistently with the $Im\bar{3}$ crystal phase. Neither evidence of structural phase transition, nor metalization was found in the explored pressure range from Raman and optical absorption spectroscopy. We show that all Raman peaks undergo continuous blueshifts with pressure, whereas the Raman spectra preserve the

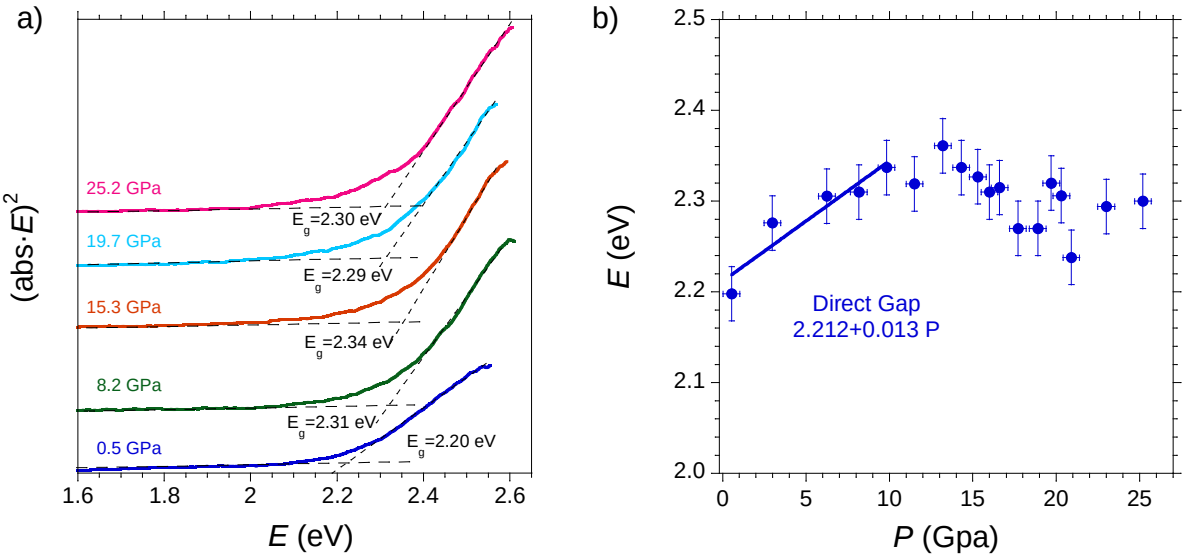

Figure 3. a) Variation of the CCTO absorption spectrum near the band-gap edge with pressure. The absorption spectra are vertically displaced to allow comparison for different pressures. The direct band-gap energy was derived by plotting (absorption$\times h\nu)^2$ vs. $h\nu$ through the interception of straight lines corresponding to the absorption edge and the zero-absorption background. b) Variation of the charge-transfer direct band gap with pressure. Note the band-gap blueshift of 13 meV GPa^{-1} from 0 to 10 GPa, and the constant value –within 0.1 eV– of $E_g = 2.3$ eV above 10 GPa.

eight-peak ambient-pressure structure in the whole pressure range. The obtained Grüneisen parameters for the stretching vibrations suggest that Ti-O bonds in CCTO are slightly tougher than those in TiO_2 in both rutile and anatase phases. The diffuse reflectance spectrum allows us to identify the different charge-transfer band components from mainly O^{2-} valence band states to conduction band states involving mainly low-energy Cu^{2+} (2-3 eV) and high-energy Ti^{4+} (> 3 eV) $3d$ orbitals. We also demonstrate that the high stability of the $Im\overline{3}$ phase with pressure up to 25 GPa, is accompanied by concomitant band gap stability, the energy of which increases slightly with pressure at 13 meV GPa^{-1} up to 10 GPa, whereas it remains as $E_g = 2.30 \pm 0.06$ eV at higher pressures. Thus, no evidence of pressure-induced metallization was found in the explored range.

Acknowledgements
This work has been supported by the Spanish Ministerio de Ciencia, Innovación y Universidades (Projects MAT2015-69508-P, PGC2018-101464-B-I00 and MALTA-Consolider Team RED2018-102612-T). E.J. thanks for an FPI research grant (Ref. BES-2016-077449).

References
[1] Subramanian M A, Li D, Duan N, Reisner B A and Sleight, A W J 2000 *Solid State Chem.* **151** 323–325
[2] Ramirez A P, Subramanian M A, Gardel M, Blumberg G. and Li D, Vogt T and Shapiro SM 2000 *Solid State Commun* **115** 217–220
[3] Homes C C, Vogt T, Shapiro S M, Wakimoto, S and Ramirez A P 2001 *Science* **293** 673-676
[4] Kolev N, Bontchev R P, Jacobson A J, Popov V N, Hadjiev V G, Litvinchuk A P and Iliev M N 2002 *Phys. Rev. B* **66** 132102
[5] He L, Neaton J B, Cohen M H, Vanderbilt D and Homes C C 2002 *Phys. Rev. B* **65** 214112
[6] He L, Neaton J B, Cohen M H and Vanderbilt D 2003 *Phys. Rev. B* **67** 012103

[7] Tselev A, Brooks C M, Ramesh R, Subramanian M A, Zheng H and Anlage SM 2003 *Tech. Rep.*
[8] Clark J H, Dyer M S, Palgrave R G, Ireland C P, Darwent J R, Claridge J B and Rosseinsky M J 2010 *J. Am. Chem. Soc.* **133** 1016-1032
[9] Valim D, Souza F A G, Freire P T C, Fagan S B, Ayala A P, Mendes F J, Almeida A F L, Fechine P B A, Sombra A S B, Olsen J S and others 2004 *Phys. Rev. B* **70** 132103
[10] Wang B, Pu YP, Wu HD, Chen K and Xu N 2013 *Ceram. Int.* **39** S525-S528
[11] Liu P, Lai Y, Zeng Y, Wu S, Huang Z and Han J 2015 *J. Alloy Compd.* **650** 59-64
[12] Klotz S, Chervin J C, Munsch P and Le Marchand G 2009 *J. Phys. D* **42** 075413
[13] Moral B A and Rodríguez F 1995 *Rev. Sci. Instrum.* **66** 5178-5182
[14] K. Syassen 2008 *High Press. Res.* **28** 75-126
[15] Barreda-Argüeso J A and Rodríguez F 2015 *F. Patent No. PCT/ES2014/000049.*
[16] Ramírez M A, Parra R, Reboredo M M, Varela J A, Castro M S and Ramajo L 2010 *Mater. Lett.* **64** 1226-1228
[17] Sekiya T, Ohta S, Kamei S, Hanakawa M and Kurita S 2001 *J. Phys. Chem. Solids* **62** 717-721
[18] Swamy V, and Dubrovinsky Leonid S 2001 *J. Phys. Chem. Solids* **62** 673-675
[19] Hong M, Dai L, Li H, Hu H, Liu K, Yang L and Pu C 2019 *Minerals* **9** 441.
[20] Mammone J F, Sharma S K and Nicol M 1980 *Solid State Commun.* **34** 799-802
[21] Hazen R M and Finger L W 1981 *J. Phys. Chem. Solids* **42** 143-151
[22] Fagan S B, Souza F A G, Ayala A P and Mendes F J 2005 *Physical Review B* **72** 014106
[23] Tyagi S, Sharma G and Sathe V G 2017 *Solid State Communications* **251** 94-97